Inorganic Chemistry

Article

pubs.acs.org/IC

$ZnGa_{2-x}In_xS_4$ ($0 \le x \le 0.4$) and $Zn_{1-2y}(CuGa)_yGa_{1.7}In_{0.3}S_4$ ($0.1 \le y \le 0.2$): Optimize Visible Light Photocatalytic H_2 Evolution by Fine Modulation of Band Structures

Jia Yang, Hao Fu, Dingfeng Yang, Wenliang Gao, Rihong Cong,* and Tao Yang*

College of Chemistry and Chemical Engineering, Chongqing University, 174 Shazhengjie Street, Chongqing 400044, People's Republic of China

Supporting Information

ABSTRACT: Band structure engineering is an efficient technique to develop desired semiconductor photocatalysts, which was usually carried out through isovalent or aliovalent ionic substitutions. Starting from a UV-activated catalyst $ZnGa_2S_4$, we successfully exploited good visible light photocatalysts for H_2 evolution by In^{3+}-to-Ga^{3+} and (Cu^+/Ga^{3+})-to-Zn^{2+} substitutions. First, the bandgap of $ZnGa_{2-x}In_xS_4$ ($0 \le x \le 0.4$) decreased from 3.36 to 3.04 eV by lowering the conduction band position. Second, $Zn_{1-2y}(CuGa)_yGa_{1.7}In_{0.3}S_4$ (y = 0.1, 0.15, 0.2) provided a further and significant red-shift of the photon absorption to ~500 nm by raising the valence band maximum and barely losing the overpotential to water reduction. $Zn_{0.7}Cu_{0.15}Ga_{1.85}In_{0.3}S_4$ possessed the highest H_2 evolution rate under pure visible light irradiation using S^{2-} and SO_3^{2-} as sacrificial reagents (386 μmol/h/g for the noble-metal-free sample and 629 μmol/h/g for the one loaded with 0.5 wt % Ru), while the binary hosts $ZnGa_2S_4$ and $ZnIn_2S_4$ (synthesized using the same procedure) show 0 and 27.9 μmol/h/g, respectively. The optimal apparent quantum yield reached to 7.9% at 500 nm by tuning the composition to $Zn_{0.6}Cu_{0.2}Ga_{1.9}In_{0.3}S_4$ (loaded with 0.5 wt % Ru).

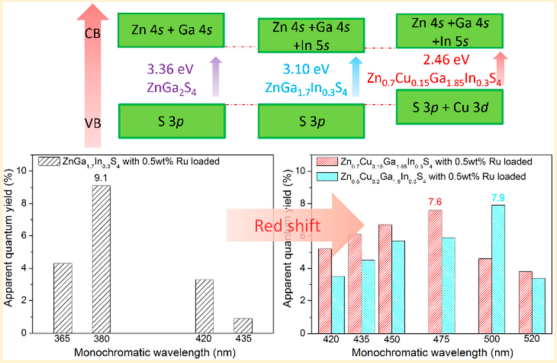

INTRODUCTION

Hydrogen generation utilizing solar energy driven photocatalysts has been recognized as a green and promising way to produce clean energy and solve the fossil fuels shortage problem.[1] During the past few decades, many photocatalysts have been developed for H_2 generation through water splitting. For example, TiO_2[2,3] and ZnO[4,5] are typical wide bandgap semiconductors and need to be activated by ultraviolet (UV) light, which, however, occupies only 5% of the solar energy; therefore, searching for visible-light-driven photocatalysts is always desired.

Metal sulfides have been widely studied as excellent photocatalysts in the visible light range because the valence bands (VBs) were mainly contributed by the S 3p orbitals instead of O 2p in oxides, resulting in higher VB maxima and narrower bandgaps.[6,7] For example, CdS is probably one of the most widely studied metal sulfides as a photochemical water reduction catalyst because of its narrow bandgap (2.4 eV) and appropriate electrochemical potentials.[8−10] However, the drawback is also apparent that metal sulfides are not capable of pure water splitting because of the inevitable photocorrosion, which can be solved by using Na_2S and Na_2SO_3 as sacrificial regents. Though metal sulfides are usually not suitable photocatalysts for pure water splitting, people could use them for photocatalytic H_2 production and, in the meantime, consume sulfur compounds from chemical industries or natural resources.

People could either use a visible light responsive metal sulfide directly, or modify a UV-light catalyst by band structure engineering strategy. Very recently, A. Kudo and H. Kaga reported solid solutions between defect chalcopyrite $ZnGa_2S_4$ and chalcopyrite $CuGaS_2$, which is in fact a cosubstitution of Cu^+/Ga^{3+} to Zn^{2+}.[11] The bandgap of $ZnGa_2S_4$ can be significantly narrowed (from 3.4 to 2.5 eV) because the incorporation of Cu 3d orbitals largely raised the VB potential. The best performance of H_2 evolution was obtained on $Zn_{0.4}(CuGa)_{0.3}Ga_2S_4$ loaded with 0.5 wt % Pd, where the apparent quantum yield (AQY) is 15% at 420 nm.

As for AQYs, there is an amazing record of 93% at 420 nm for the Pt-PdS/CdS catalyst reported by C. Li et al.[12] In addition, $ZnIn_2S_4$, although possessing a different structure with $ZnGa_2S_4$ (see Figure S1 in the Supporting Information, SI), has been extensively investigated and the highest AQY reaches 34.3% at 420 nm.[13,14] The interesting point is that the presumably existed $ZnGa_{2-x}In_xS_4$ solid solutions should possess the bandgaps between $ZnGa_2S_4$ (~3.4 eV) and $ZnIn_2S_4$ (~2.5 eV), and the In^{3+}-to-Ga^{3+} substitution could lower the conduction band (CB) position.[15−18] Moreover, according to A. Kudo's work on $ZnGa_2S_4$−$CuGaS_2$ solid solutions, where the modification is started from the host compound $ZnGa_2S_4$, we believe that the cosubstitution of Cu^+/Ga^{3+} to Zn^{2+} on

Received: December 30, 2014
Published: February 19, 2015

DOI: 10.1021/ic503101s
Inorg. Chem. 2015, 54, 2467−2473

$ZnGa_{2-x}In_xS_4$ would further reduce the bandgap energy by raising the VB position, and allow the absorption edge to red-shift. Of course, maintaining a substantial overpotential to H^+/H_2 is also necessary during the bandgap modification.

Under such a scheme, we first designed a systematic study on the photocatalytic H_2 production of ternary metal sulfides $ZnGa_{2-x}In_xS_4$ ($0 \le x \le 0.4$). It was successful that the bandgap of UV-excited $ZnGa_2S_4$ was tuned to the visible region, and $ZnGa_{1.7}In_{0.3}S_4$ (with 0.5 wt % Ru loaded) possessed the best performance of H_2 production efficiency (205 μmol/h/g) under the light beam ≥420 nm, which is 7 times that of $ZnIn_2S_4$ prepared using the same method. On the other hand, theoretical calculations suggest that the incorporation of Cu^+ would further raise the VB potential. Therefore, a compositional modulation on $ZnGa_{1.7}In_{0.3}S_4$ by partially incorporating Cu^+/Ga^{3+} resulted in a significant red-shift of the bandgap, and the H_2 evolution rate achieved 535 μmol/h/g on $Zn_{0.7}Cu_{0.15}Ga_{1.85}In_{0.3}S_4$-0.5 wt % Ru. Moreover, the optimal AQY was regulated from 9.1% at 380 nm ($ZnGa_{1.7}In_{0.3}S_4$) to 7.6% at 475 nm ($Zn_{0.7}Cu_{0.15}Ga_{1.85}In_{0.3}S_4$), and eventually to 7.9% at 500 nm ($Zn_{0.6}Cu_{0.2}Ga_{1.9}In_{0.3}S_4$).

EXPERIMENTAL SECTION

Two series of sulfides with the formulas of $ZnGa_{2-x}In_xS_4$ ($0 \le x \le 0.4$ and $x = 2$) and $Zn_{1-2y}(CuGa)_yGa_{1.7}In_{0.3}S_4$ ($y = 0.1, 0.15, 0.2$) were prepared by typical high temperature solid state reactions. Stoichiometric amounts of ZnS, Ga_2S_3, and In_2S_3 (and Cu_2S) were mixed and ground in an agate mortar. The mixture (~0.25 g) was heated in a vacuumed tube furnace at 700 °C for 2 h. After cooling to the room temperature, the resultant products were ready for further characterizations.

The powder X-ray diffraction (XRD) patterns of the samples were performed on a PANalytical X'pert powder diffractometer equipped with a PIXcel detector and with Co Kα radiation, with the operation voltage and current maintained at 40 kV and 40 mA, respectively. Diffuse reflectance spectra were obtained with a Shimadzu UV-3600 spectrometer equipped with an integrating sphere attachment. The spectra were converted from reflectance to absorbance mode by the Kubelka–Munk method. $BaSO_4$ was used as a reflectance standard. The bandgap energies were estimated according to the peaks of the differential curves of absorption spectra.

Photocatalytic activities were tested on a gas-closed circulation system equipped with a vacuum line (CEL-SPH2N system), a reaction vessel, and a gas sampling port that is directly connected to a gas chromatograph (Shanghai Techcomp-GC7900, TCD detector, molecular sieve 5A, N_2 gas carrier). In a typical run, 50 mg of a catalyst was dispersed by a magnetic stirrer in 50 mL of an aqueous solution containing 0.1 mol L^{-1} Na_2S and 0.5 mol L^{-1} Na_2SO_3 in a 150 mL Pyrex glass reactor with a quartz cover. The solution was kept stirring, and a 10 °C recycling water bath was applied to keep the reaction vessel at a constant temperature. The light irradiation source was generated by an external 300W Xe-lamp (CEL-HXF300, Beijing AuLight) with or without a (cutoff or bandpass) filter laid on the top of the reaction vessel.

The Ru cocatalyst loading was performed in a photodeposition method using the above setup. For example, 0.25 g of catalyst together with 0.5 wt % Ru aqueous solution (0.975 mg/mL for Ru^{3+}) were added into 50 mL of 0.1 M Na_2S and 0.5 M Na_2SO_3 aqueous solution. The suspension was irradiated for 1 h using a 300 W Xe-lamp. Then, the powder sample was collected and washed by deionized water.

Apparent quantum yield (AQY) for H_2 evolution under a monochromatic irradiation was determined according to

$$\mathrm{AQY}(\%) = \frac{\text{number of reacted electrons}}{\text{number of incident phtotons}} \times 100$$

The number of reacted electrons related to the H_2-production rate, and the number of incident photons, can be measured by the Si-photodiode. More detailed calculations are described below.

$$A_R = \pi R^2$$

A_R represents irradiated area, and R represents radius of reaction vessel, which is 2.5 cm.

$$P = \bar{E} \cdot A_R$$

P represents incident photon flux, and $\bar{E}$ represents average irradiance.

$$N_P^i = \frac{Pt\lambda}{hc}$$

The abbreivations correspond to the following: N_P^i, incident photon number; t, time; λ, wavelength; h, Planck constant; c, light velocity.

$$\mathrm{AQY} = \frac{2R_{H_2}N_A t}{N_P^i}$$

R_{H_2} indicates H_2 evolution rate, and N_A represents Avogadro's constant.

Theoretical studies on $ZnGa_2S_4$ and $CuGaS_2$ are operated by the Vienna ab initio simulation package (VASP).[19] The projector augmented-wave (PAW) method[20] implemented in the VASP code was utilized to describe the interaction between the ionic cores and the valence electrons. The generalized gradient approximation (GGA) parametrized by Perdew, Burke, and Ernzerhof (PBE)[21] was employed to describe the exchange-correlation potential in the standard DFT calculations. For single point energy and density of states, a cutoff energy of 500 eV for the plane-wave basis and 9 × 9 × 9 Monkhorst–Pack G-centered k-point meshes were employed. The band structures $E(k)$ were computed on a discrete k mesh along with high-symmetry directions. Each interval between two adjacent high symmetry points was divided into 100 parts equally. For example, for $CuGaS_2$, from the G point with the coordinates (0, 0, 0) to the Z point (0.0, 0.0, 0.5), A point (0.5, 0.5, 0.5), M point (0.5, 0.5, 0.0), R point (0.0, 0.5, 0.5), and X point (0.0, 0.5, 0.0) in units of ($2\pi/a$, $2\pi/b$, $2\pi/c$).

RESULTS AND DISCUSSION

Synthesis and Phase Identification. The syntheses of $ZnGa_{2-x}In_xS_4$ were successful when $0 \le x \le 0.4$. Powder XRD patterns of as-prepared $ZnGa_{2-x}In_xS_4$ are basically the same. All match well with the reference pattern of the defect chalcopyrite $ZnGa_2S_4$ (see Figure 1a). A slight left-shift of the refection peaks can be observed, especially for the (220) and (204) peaks at ~57.5°/2θ, indicating the unit cell expansion induced by the In^{3+}-substitution. More accurate unit cell determination was performed by Le Bail refinements on powder XRD patterns using TOPAS,[22] and the refined cell parameters are shown in Figure 1b. The linear increase of the length for a-, c-axes as well as the cell volume (see Figure 1a) along with the increase of x is solid evidence for the successful syntheses of pure $ZnGa_{2-x}In_xS_4$ ($0 \le x \le 0.4$). Further increasing the In^{3+}-concentration in the starting material would not give a larger cell lattice; instead, an impurity phase $(Ga,In)_2S_3$ appears. Then it is conclusive that the upper limit of the In^{3+}-doping is around x = 0.4, which is 20 atom %. $ZnIn_2S_4$ was also prepared at the same condition, whose powder XRD pattern is consistent with the reference (see Figure S2, Supporting Information).

At the beginning we had assumed there existed a wide range of solid solutions between $ZnGa_2S_4$ and $ZnIn_2S_4$. Apparently, it is not the case experimentally. At a reaction temperature below 650 °C, In_2S_3 would not react with other reagents. At 650 °C, the reaction between ZnS, Ga_2S_3, and In_2S_3 could proceed but in a very slow speed and incomplete even after a long period of time. So the final reaction temperature was selected to be 700

DOI: 10.1021/ic503101s
Inorg. Chem. 2015, 54, 2467–2473

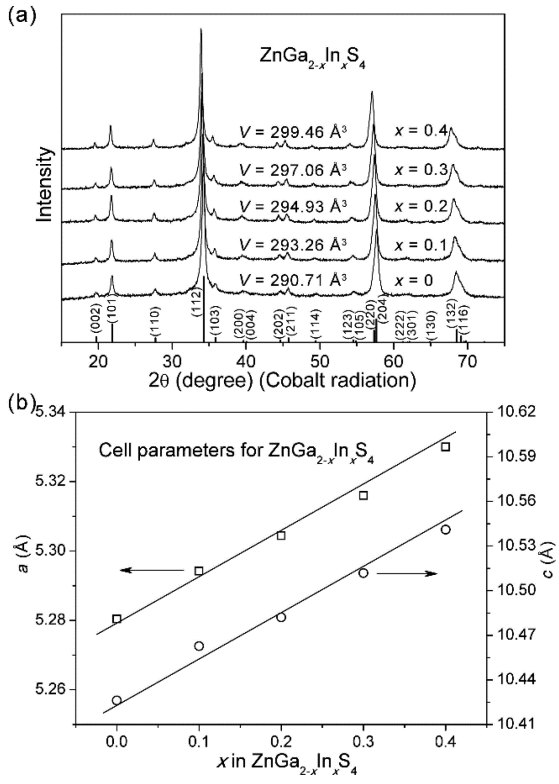

Figure 1. (a) Powder XRD patterns for $ZnGa_{2-x}In_xS_4$ solid solutions with the reference pattern shown below. (b) The refined cell parameters from Le Bail refinements.

°C, at which the reaction was completed in just 2 h. At 700 °C, $ZnGa_{1.6}In_{0.4}S_4$ is thermodynamically stable, while "$ZnGa_{1.5}In_{0.5}S_4$" is not. This is the major reason why there was the impurity $(Ga,In)_2S_3$ when $x = 0.5$. Hypothetically, a higher reaction temperature, i.e., 750 °C, might raise the In^{3+}-doping upper limit. However, In_2S_3 would volatilize at the heating zone of the vacuumed tube furnace, and transfer to and solidify at the cold end of the tube. The volatilization of In_2S_3 may partially be solved if performing the syntheses in a small and sealed quartz tube, like that in the syntheses of $Zn_{1-2x}(CuGa)_xGa_2S_4$.[11]

It will be shown later that the $ZnGa_{1.7}In_{0.3}S_4$ possesses the best photocatalytic performance of water reduction. As a consequence, we incorporated $CuGaS_2$ into this specific composition, forming $Zn_{1-2y}(CuGa)_yGa_{1.7}In_{0.3}S_4$ (y = 0.1, 0.15, 0.2). The corresponding powder XRD patterns are shown in Figure 2. The cell volume decreases when y increases, which is as expected due to the replacement of Zn^{2+} by smaller cations (i.e., Zn^{2+}, 0.60 Å; Cu^+, 0.60 Å; Ga^{3+}, 0.47 Å). Finally, all the used catalysts show the same powder XRD patterns with those of as-synthesized samples, indicating the stability in our photocatalytic conditions (see Figure S3, Supporting Information).

Band Structure Engineering. In order to rationally perform an effective strategy on band structure engineering, the electronic band structures of $ZnGa_2S_4$ and $CuGaS_2$ along the symmetry lines in the Brillouin zone of the unit cell were calculated as plotted in Supporting Information Figure S4. Both structures have a direct bandgap (2.34 eV, and 1.21 eV, respectively). Figure 3 gives the total and partial density of states (DOS and PDOS) projected on the constituent atoms in both compounds. For the parent compound $ZnGa_2S_4$, the bottom of the CB was determined by the 4s orbitals of Zn^{2+},

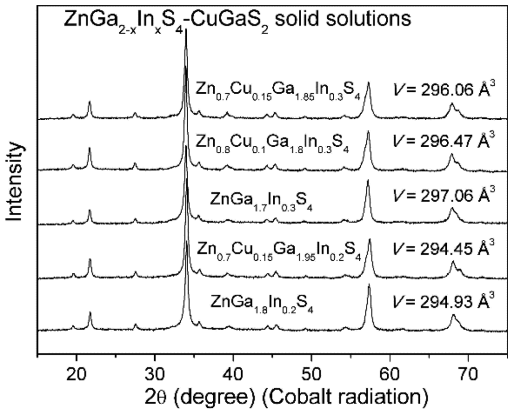

Figure 2. Powder XRD patterns for $Zn_{2-2y}(CuGa)_yGa_{1.7}In_{0.3}S_4$ and the refined cell volumes for as-synthesized samples.

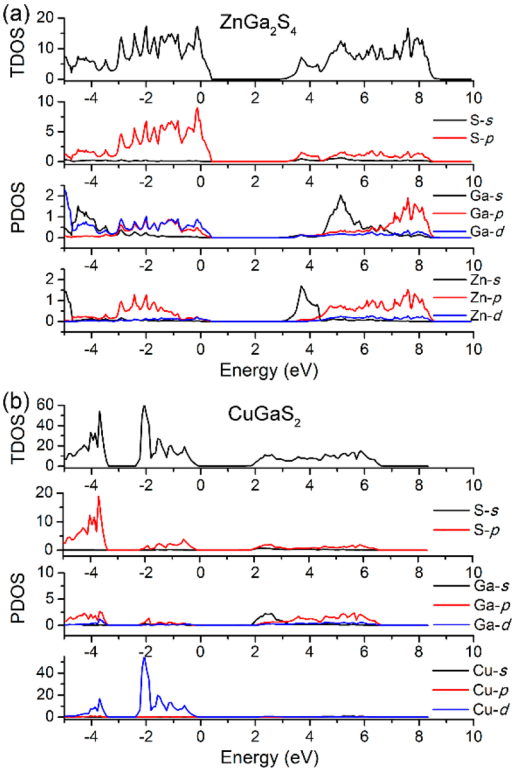

Figure 3. Total and partial density of states of (a) $ZnGa_2S_4$ and (b) $CuGaS_2$.

while the 4s orbitals of Ga^{3+} contribute to a relatively higher position of the CB. The top of the VB was mostly composed of the 3p orbitals of S^{2-} as expected. $CuGaS_2$ has a narrower bandgap, where the CB was determined by the 4s orbitals of Ga^{3+} and the VB was composed of both 3p orbitals of S^{2-} and 3d orbitals of Cu^+.

As stated in the Introduction, the band structure modification is the key technique to develop a visible light photocatalyst based on a UV-responsive host. The bandgaps of the ternary metal sulfides $ZnGa_{2-x}In_xS_4$ ($0 \le x \le 0.4$ and $x = 2$) were estimated by the diffuse reflectance spectra (see Table 1 and Figure 4). All these samples have a very sharp absorption edge, confirming again that homogeneous solid solutions were successfully established. The two end members have their usual bandgap energies, i.e., 3.36 eV for $ZnGa_2S_4$ and 2.55 eV for $ZnIn_2S_4$. The bandgap decreases from 3.27 eV at $x = 0.1$ to 3.04

DOI: 10.1021/ic503101s
Inorg. Chem. 2015, 54, 2467−2473

Table 1. Summary of Band Gap Energies and H_2 Evolution Rates (μmol/h/g) for Studied Samples[a]

sample	band gap (eV)	Xe lamp	≥420 nm
$ZnGa_2S_4$	3.36	447(10)	0
$ZnGa_{1.9}In_{0.1}S_4$	3.27	489(9)	13.6(0.2)
$ZnGa_{1.8}In_{0.2}S_4$	3.18	529(4)	45.6(0.9)
$ZnGa_{1.7}In_{0.3}S_4$	3.10	933(12)	115.5(0.9)
$ZnGa_{1.6}In_{0.4}S_4$	3.04	617(6)	77.3(0.9)
$ZnIn_2S_4$	2.55	72(1)	27.9(0.5)
$ZnGa_{1.7}In_{0.3}S_4$-0.5 wt % Ru		2156(19)	205(6)
$Zn_{0.8}Cu_{0.1}Ga_{1.8}In_{0.3}S_4$	2.62	386(8)	169(1)
$Zn_{0.7}Cu_{0.15}Ga_{1.85}In_{0.3}S_4$	2.46	629(13)	386(12)
$Zn_{0.6}Cu_{0.2}Ga_{1.9}In_{0.3}S_4$	2.44	326(8)	267(5)
$Zn_{0.7}Cu_{0.15}Ga_{1.85}In_{0.3}S_4$-0.5 wt % Ru		1154(34)	535(8)
$Zn_{0.6}Cu_{0.2}Ga_{1.9}In_{0.3}S_4$-0.5 wt % Ru		800(23)	491(15)

[a] Photocatalytic condition, 50 mg of photocatalyst, 50 mL of S^{2-}/SO_3^{2-} aqueous solution (0.5 M Na_2SO_3, 0.1 M Na_2S).

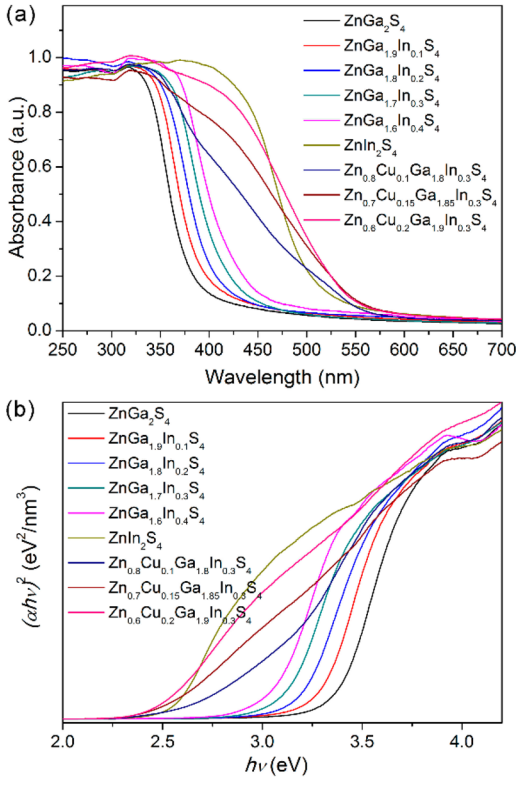

Figure 4. (a) UV−vis diffuse reflectance spectra of all studied samples. (b) Estimated band gap energy E_g with plots of $(\alpha h\nu)^2$ against photon energy ($h\nu$).

eV when $x = 0.4$. It should be noted that the calculated bandgap is usually smaller than the experimental value due to the discontinuity of XC energy.

In fact, the first step of narrowing bandgaps, which is caused by the lowering of the CB potential through In^{3+}-to-Ga^{3+} substitution, is moderate. It can be understood that the bottom of the CB was mostly composed of the 4s orbitals of Zn^{2+}; thus, the substitution of the Ga^{3+} by In^{3+} gives only a minor change of the potential of CB. Even with $x = 0.4$, the absorption edge is still close to the UV−vis boundary. Obviously, it is favored if a photocatalyst can be responsive to the strongest emission (~500 nm) of the solar spectrum. So, addition efforts are needed to further shift the absorption edge to a higher wavelength.

On the basis of the PDOS analyses, an incorporation of $CuGaS_2$ into the framework of $ZnGa_2S_4$ is supposed to increase the top of the VB. Experimentally, A. Kudo et al. have indeed proved that the Cu^+/Ga^{3+} cosubstitution to Zn^{2+} in a defect chalcopyrite structure could significantly narrow the bandgaps by elevating the VB position.[11] In their study, the maximum AQY was achieved to 15% but at a relative low wavelength beam, 420 nm. Here, in our study, we carried out the same Cu^+/Ga^{3+} cosubstitution on a selected compound $ZnGa_{1.7}In_{0.3}S_4$, because its bandgap was already narrowed comparing to $ZnGa_2S_4$ and it in fact has the highest H_2 evolution rate both under Xe-lamp and pure visible light (≥420 nm) irradiations when compared to other $ZnGa_{2-x}In_xS_4$ samples.

Three quaternary metal sulfides ($Zn_{1-2y}(CuGa)_yGa_{1.7}In_{0.3}S_4$, $y = 0.1, 0.15, 0.2$) were therefore prepared and evaluated. As shown in Table 1 and Figure 4, the bandgaps are 2.62, 2.46, and 2.44 eV, respectively. First, it is remarkable that doping a small amount of Cu^+ would greatly reduce the bandgap energy from 3.1 to ~2.5 eV.

Second, though the bandgaps seem to be mathematically close, when changing the substitution level of $CuGaS_2$, the photon absorption behaviors are quite different. For example, as shown in Figure 4a, the absorbances at 475 nm for $Zn_{0.6}Cu_{0.2}Ga_{1.9}In_{0.3}S_4$ and $Zn_{0.8}Cu_{0.1}Ga_{1.8}In_{0.3}S_4$ are 0.71 and 0.42, respectively; therefore, we speculate that the absorption coefficient of $Zn_{0.6}Cu_{0.2}Ga_{1.9}In_{0.3}S_4$ during the photocatalytic reaction is ~70% higher than that of the latter one. Such a difference can lead to a substantial red-shift in wavelength of the optimal absorption, which is of course desired for solar energy conversion.

Third, the bandgaps of three quaternary sulfides are comparable to that of the $ZnIn_2S_4$. Then, people may think that it seems unnecessary to produce a complex composition. In fact, $ZnIn_2S_4$ has already been widely investigated to be a good photocatalyst for H_2 production, because of its appropriate bandgap.[23−25] However, the CB minimum, which is contributed by In^{3+} 4d orbitals, is relatively low to provide a large overpotential to water reduction. As shown in Table 1, the bandgap of $ZnIn_2S_4$ (2.55 eV) is smaller than that of $ZnGa_2S_4$ (3.36 eV), while the H_2 evolution rate of $ZnGa_2S_4$ is 5 times higher than that of $ZnIn_2S_4$ under Xe lamp irradiation. This is an indication about the insufficient overpotential of CB minimum for $ZnIn_2S_4$ versus H^+/H_2 in this photocatalytic condition. Here this disadvantage was significantly improved by our band structure engineering. Our current quaternary metal sulfides $Zn_{1-2y}(CuGa)_yGa_{1.7}In_{0.3}S_4$ ($y = 0.1, 0.15, 0.2$) were rationally designed and synthesized in order to provide not only a suitable bandgap for a high level of energy absorption, but also a sufficiently negative CB position for H_2 production. This point will be proved by the photocatalytic efficiency shown in a later section.

In summary, the overall band structure engineering strategy was schemed in Figure 5. We first slightly reduce the CB by a partial doping of In^{3+} into $ZnGa_2S_4$ without changing the VB potential. $ZnGa_{1.7}In_{0.3}S_4$ (with a bandgap of 3.10 eV) was further modified by Cu^+/Ga^{3+}-to-Zn^{2+} cosubstitution, which leads to a significant decrease of the bandgap (2.46 eV for $Zn_{0.7}Cu_{0.15}Ga_{1.85}In_{0.3}S_4$) mainly by elevating the VB potential.

DOI: 10.1021/ic503101s
Inorg. Chem. 2015, 54, 2467−2473

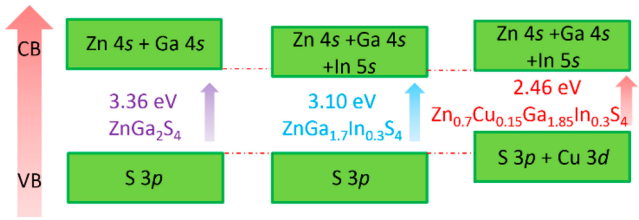

Figure 5. Overall band structure engineering strategy in this work.

Photocatalytic Activities of $ZnGa_{2-x}In_xS_4$ ($0 \le x \le 0.4$). Table 1 summarizes the photocatalytic H_2 evolution from an aqueous solution containing Na_2S and Na_2SO_3 as electron donors using as-synthesized metal sulfides under both Xe-lamp and pure visible light (≥420 nm) irradiations. Detailed H_2 production curves were given in the Supporting Information. $ZnGa_2S_4$ has a moderate activity under Xe-lamp irradiation, but zero activity when irradiated by pure visible light, which is consistent with its wide bandgap character. By doping with In^{3+}, all the $ZnGa_{2-x}In_xS_4$ ($0 \le x \le 0.4$ and $x = 2$) samples are capable of absorbing visible light photons and show pure visible light activities. As shown in Figure 6, the optimal composition is $ZnGa_{1.7}In_{0.3}S_4$, for which the H_2 evolution rates are 933 and 115.5 μmol/h/g under Xe-lamp and pure visible light, respectively.

The In^{3+}-doping narrows the bandgap, allowing more photons to be absorbed, which is a positive factor; on the other hand, it also lowers the CB potential, reducing the overpotential to water reduction, which is a negative factor. The $ZnGa_{1.7}In_{0.3}S_4$ is experimentally the best catalyst to possess a good balance between these two factors. Moreover, the pure visible light H_2 production efficiency of $ZnIn_2S_4$, which has a very narrow bandgap (2.55 eV), is only 25% of that for $ZnGa_{1.7}In_{0.3}S_4$. This has already been explained in preceding sections that the CB potential also matters during photocatalytic water reduction.

Experimentally, loading an appropriate cocatalyst is a powerful method to enhance the photocatalytic activity by extending the lifetime of photogenerated charge carriers. As shown in Table 1, $ZnGa_{1.7}In_{0.3}S_4$ with 0.5 wt %-Ru loaded shows a nearly doubled H_2 production rate under both irradiation conditions (2156 and 205 μmol/h/g, respectively). AQYs under various monochromatic lights on this sample (as shown in Figure 6c and Supporting Information Table S1) allow us to evaluate the intrinsic photocatalytic ability. The highest H_2 evolution rate was observed to be 295.1 μmol/h/g at 380 nm with an AQY of 9.1%. It is barely on the edge of visible light region. The AQYs at 420 and 435 nm are only 3.3% and 0.9%, pointing out that this sample is not a good visible light photocatalyst. Indeed, the H_2 evolution rate irradiated by beam ≥420 nm is only ~10% of that by Xe-lamp, indicating that the majority of the H_2 production comes from the UV-light irradiation.

Photocatalytic Activities of $Zn_{1-2y}(CuGa)_yGa_{1.7}In_{0.3}S_4$ ($0.1 \le y \le 0.2$). $ZnGa_{1.7}In_{0.3}S_4$ is not an intrinsically visible light photocatalyst but is a good host for further modifications. As shown in Table 1, though the H_2 evolution rates for $Zn_{1-2y}(CuGa)_yGa_{1.7}In_{0.3}S_4$ ($y = 0.1, 0.15, 0.2$) are not as high as that of $ZnGa_{1.7}In_{0.3}S_4$ under Xe-lamp irradiation, they give much higher pure visible light activities, especially with $Zn_{0.7}Cu_{0.15}Ga_{1.85}In_{0.3}S_4$ showing the highest rate of 386 μmol/h/g. When it was loaded with 0.5 wt %-Ru, the H_2 evolution rates increase to 1154 and 535 μmol/h/g, respectively (see

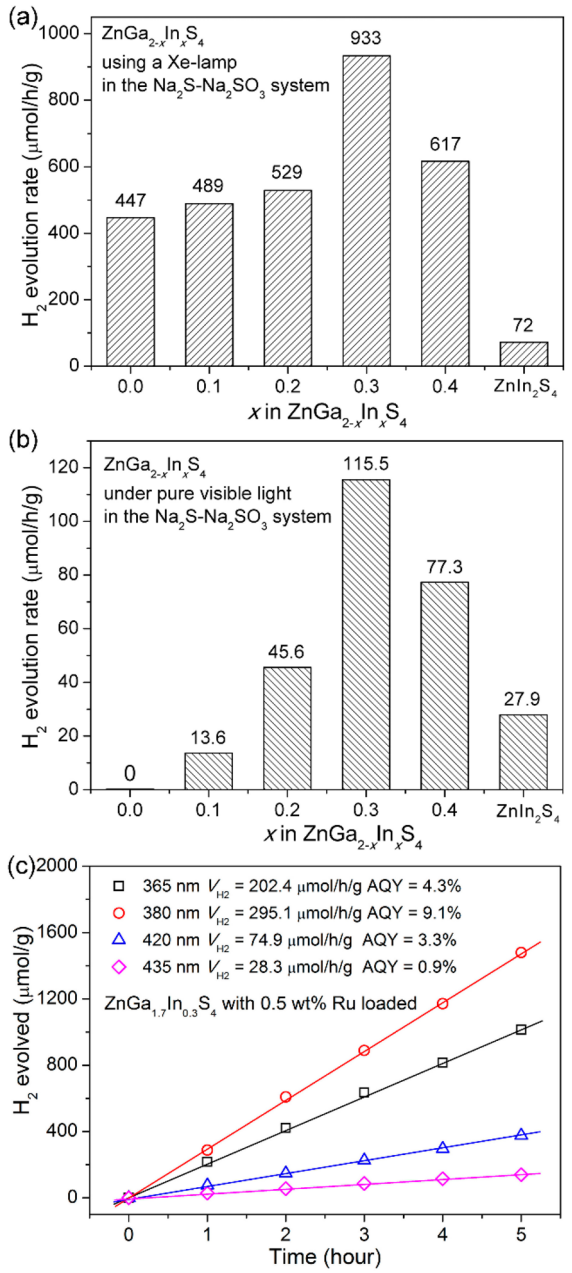

Figure 6. Photocatalytic H_2 evolution rates for $ZnGa_{2-x}In_xS_4$ under (a) Xe-lamp and (b) pure visible light irradiation. (c) Photocatalytic H_2 evolution under monochromatic lights and corresponding apparent quantum yields for $ZnGa_{1.7}In_{0.3}S_4$ with 0.5 wt % Ru loaded. Photocatalytic condition, 50 mg of photocatalyst, 50 mL of S^{2-}/SO_3^{2-} aqueous solution (0.5 M Na_2SO_3, 0.1 M Na_2S).

Table 1). Monochromatic light with six different wavelengths were applied on this 0.5 wt % Ru-loaded $Zn_{0.7}Cu_{0.15}Ga_{1.85}In_{0.3}S_4$. The optimal H_2 evolution rate (185.6 μmol/h/g) and AQY (7.6%) were observed at 475 nm (see Figure 7a and Supporting Information Table S2), which shows a 95 nm red-shift compared to $ZnGa_{1.7}In_{0.3}S_4$ (380 nm).

It is interesting to look at the activity of $Zn_{0.6}Cu_{0.2}Ga_{1.9}In_{0.3}S_4$. For example, it does not have an H_2 production rate as high as that of $Zn_{0.7}Cu_{0.15}Ga_{1.85}In_{0.3}S_4$, but it has a higher efficiency of photon absorbance at a longer wavelength according to the reflectance spectra. The AQYs for $Zn_{0.6}Cu_{0.2}Ga_{1.9}In_{0.3}S_4$-0.5 wt % Ru sample are 5.7%, 5.9%, 7.9%, and 3.4%

DOI: 10.1021/ic503101s
Inorg. Chem. 2015, 54, 2467−2473

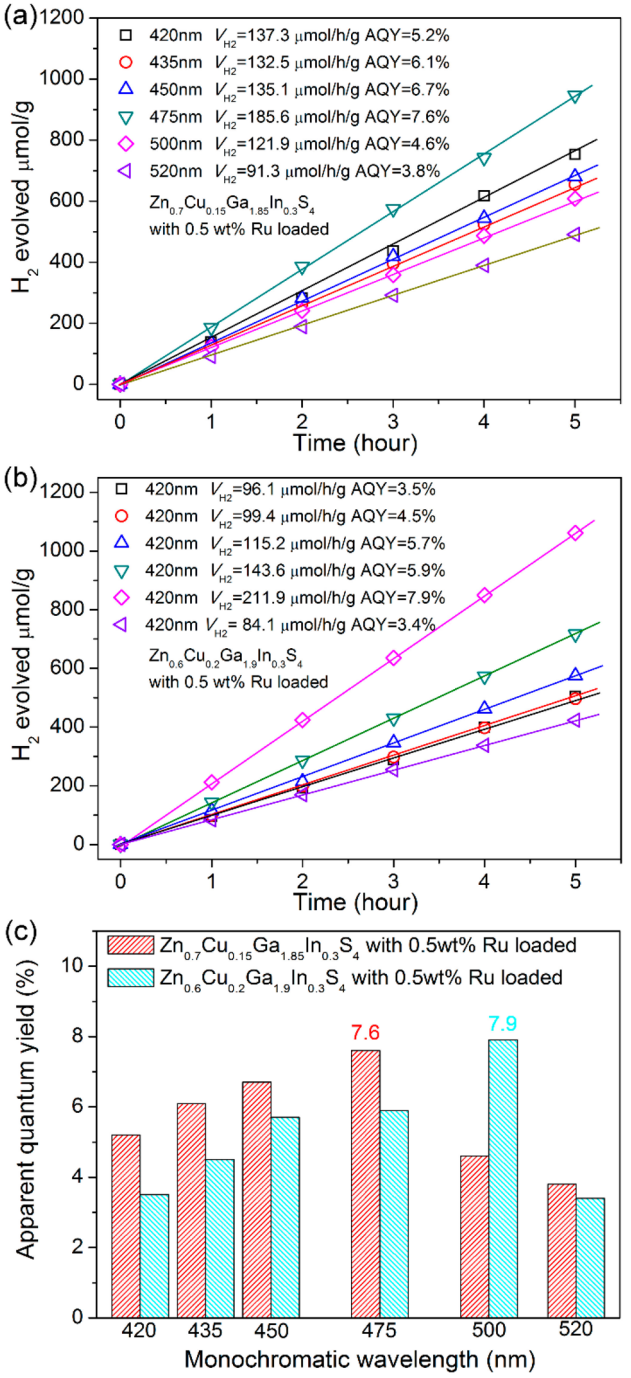

Figure 7. Photocatalytic H_2 evolution under monochromatic lights for (a) $Zn_{0.7}Cu_{0.15}Ga_{1.85}In_{0.3}S_4$ and (b) $Zn_{0.6}Cu_{0.2}Ga_{1.9}In_{0.3}S_4$ with 0.5 wt % Ru loaded. (c) Corresponding apparent quantum yields for both sulfides. Photocatalytic condition, 50 mg of photocatalyst, 50 mL of S^{2-}/SO_3^{2-} aqueous solution (0.5 M Na_2SO_3, 0.1 M Na_2S).

at 450, 475, 500, and 520 nm, respectively (see Figure 7b and Supporting Information Table S3). The red-shift of the optimal wavelength compared to $Zn_{0.7}Cu_{0.15}Ga_{1.85}In_{0.3}S_4$ is ~25 nm.

We need to compare the photocatalytic activities of quaternary metal sulfides to that of $ZnGa_{1.7}In_{0.3}S_4$. According to our initial idea, such Cu^+/Ga^{3+} codoping strategy into the host compound would significantly decrease the bandgap by raising the VB potential, but barely lose the CB overpotential to water reduction. Then, the photocatalytic H_2-production rates should be much higher than that of $ZnGa_{1.7}In_{0.3}S_4$. However, it is not exactly consistent with the experimental results; i.e., the activities under Xe-light irradiation for all quaternary metal sulfides are well below our expectation. We speculate that the photoexcited e^- and h^+ have a relatively more severe problem of bulk recombination than those in ternary metal sulfides. The charge carrier is h^+ considering that both $ZnGa_2S_4$ and $CuGaS_2$ are p-type semiconductors. In these quaternary metal sulfides, Cu^+ cations serve as hole-trapping centers, which are obstacles to the itinerating of h^+ and lead to bulk-type e^-–h^+ recombinations. Under such a scenario, it is understandable that quaternary metal sulfides have less efficiency in charge separation and thus show low activities under Xe-light. The enhancements of the H_2-production under pure visible light irradiation are caused by the narrowing of the bandgaps, which would create many more photoexcitons.

We performed a prolonged experiment on the representative catalyst $Zn_{0.7}Cu_{0.15}Ga_{1.85}In_{0.3}S_4$ under the visible light ($\lambda \geq 420$ nm). After being irradiated for 3 h, the system was vacuumed to remove the produced H_2 and started over. After six cycles, with the photocatalytic activity being kept constant (see Figure S10, Supporting Information), no obvious difference can be observed from XRD. It can be concluded that the studied metal sulfides here are reasonably stable.

CONCLUSION

In conclusion, we successfully modulated the band structure of $ZnGa_2S_4$ by In^{3+}-to-Ga^{3+} and Cu^+/Ga^{3+}-to-Zn^{2+} substitutions. The former reduced the bandgap energy from 3.36 to 3.04 eV by lowering the CB position, and the latter further narrowed the bandgap to ~2.5 eV by raising the VB maximum. $ZnGa_{1.7}In_{0.3}S_4$ gave the highest photocatalytic efficiency in $ZnGa_{2-x}In_xS_4$ ($0 \leq x \leq 0.4$) solid solutions, and the optimal AQY is 9.1% at 380 nm. Among $Zn_{1-2y}(CuGa)_yGa_{1.7}In_{0.3}S_4$ (y = 0.1, 0.15, 0.2), $Zn_{0.7}Cu_{0.15}Ga_{1.85}In_{0.3}S_4$ possessed the highest H_2 evolution rate under pure visible light irradiation (386 μmol/h/g for the noble-metal-free sample and 629 μmol/h/g for the one loaded with 0.5 wt % Ru). The optimal AQY was 7.6% at 475 nm, which is a 75 nm red-shift compared to $ZnGa_{1.7}In_{0.3}S_4$. The optimal AQY reached to 7.9% at 500 nm by tuning the composition to $Zn_{0.6}Cu_{0.2}Ga_{1.9}In_{0.3}S_4$ (loaded with 0.5 wt % Ru). Although the finally obtained AQYs are not enhanced as compared to previous work in the literature, which means further efforts would be needed, like the improvement of the particle crystallization and compact interface with the cocatalysts, current work on fine modulation of band structures proves the success of our strategy.

ASSOCIATED CONTENT

Supporting Information

Tables of AQYs, crystal structure and XRD for $ZnIn_2S_4$, XRD for all recycled photocatalysts, and photocatalytic H_2 evolution plots against time. This material is available free of charge via the Internet at http://pubs.acs.org.

AUTHOR INFORMATION

Corresponding Authors

*E-mail: congrihong@cqu.edu.cn.
*E-mail: taoyang@cqu.edu.cn.

Notes

The authors declare no competing financial interest.

DOI: 10.1021/ic503101s
Inorg. Chem. 2015, 54, 2467–2473

■ ACKNOWLEDGMENTS

This work was financially supported by the Nature Science Foundation of China (Grants 91222106, 21101175, 21171178) and Natural Science Foundation Project of Chongqing (Grants 2012jjA0438, 2014jcyjA50036). The Fundamental Research Funds for the Central Universities (Grant CQDXWL-2014-005) also partially supported this work.

■ REFERENCES

(1) Lewis, N. S. *Nature* **2001**, *414*, 589.
(2) Schrauzer, G. N.; Guth, T. D. *J. Am. Chem. Soc.* **1977**, *22*, 7189.
(3) Fujishima, A.; Honda, K. *Nature* **1972**, *238*, 37.
(4) Chen, X. B.; Shen, S. H.; Guo, L. J.; Mao, S. S. *Chem. Rev.* **2010**, *110*, 6503.
(5) Wang, X. W.; Yin, L. C.; Liu, G.; Wang, L. Z.; Saito, R.; Lu, G. Q.; Cheng, H. M. *Energy Environ. Sci.* **2011**, *4*, 3976.
(6) Ishikawa, A.; Takata, T.; Kondo, J. N.; Hara, M.; Kobayashi, H.; Domen, K. *J. Am. Chem. Soc.* **2002**, *124*, 13547.
(7) Hisatomi, T.; Kubota, J.; Domen, K. *Chem. Soc. Rev.* **2014**, *43*, 7520.
(8) Zong, X.; Yan, H. J.; Wu, G. P.; Ma, G. J.; Wen, F. Y.; Wang, L.; Li, C. *J. Am. Chem. Soc.* **2008**, *130*, 7176.
(9) Gratzel, M. *Acc. Chem. Res.* **1981**, *14*, 376.
(10) Kalyanasundaram, K.; Grätzel, M.; Pelizzetti, E. *Coord. Chem. Rev.* **1986**, *69*, 57.
(11) Kaga, H.; Kudo, A. *J. Catal.* **2014**, *310*, 31.
(12) Yan, H. J.; Yang, J. H.; Ma, G. J.; Wu, G. P.; Zong, X.; Lei, Z. B.; Shi, J. Y.; Li, C. *J. Catal.* **2009**, *266*, 165.
(13) Lei, Z. B.; You, W. S.; Liu, M. Y.; Zhou, G. H.; Takata, T.; Hara, M.; Domen, K.; Li, C. *Chem. Commun.* **2003**, 2142.
(14) Chai, B.; Peng, T. Y.; Zeng, P.; Zhang, X. H.; Liu, X. J. *J. Phys. Chem. C* **2011**, *115*, 6149.
(15) Wang, Y. H. A.; Zhang, X. Y.; Bao, N. Z.; Lin, B. P.; Gupta, A. *J. Am. Chem. Soc.* **2011**, *133*, 11072.
(16) Sun, C.; Gardner, J. S.; Long, G.; Bajracharya, C.; Thurber, A.; Punnoose, A.; Rodriguez, R. G.; Pak, J. J. *Chem. Mater.* **2010**, *22*, 2699.
(17) Ahmadi, M.; Pramana, S. S.; Xi, L. F.; Boothroyd, C.; Lam, Y. M.; Mhaisalkar, S. *J. Phys. Chem. C* **2012**, *116*, 8202.
(18) Shen, S. L.; Wang, Q. B. *Chem. Mater.* **2013**, *25*, 1166.
(19) Kresse, G.; Joubert, D. *Phys. Rev. B* **1999**, *59*, 1758.
(20) Blochl, P. E. *Phys. Rev. B* **1994**, *50*, 17953.
(21) Perdew, J. P.; Burke, K.; Ernzerhof, M. *Phys. Rev. Lett.* **1996**, *77*, 3865.
(22) Bruker, A. X. S. *TOPAS, V4.1-beta*; Bruker AXS: Karlsruhe, Germany, 2004.
(23) Shang, L.; Zhou, C.; Bian, T.; Yu, H. J.; Wu, L. Z.; Tung, C. H.; Zhang, T. R. *J. Mater. Chem. A* **2013**, *1*, 4552.
(24) Hou, J. G.; Yang, C.; Cheng, H. J.; Wang, Z.; Jiao, S. Q.; Zhu, H. G. *Phys. Chem. Chem. Phys.* **2013**, *15*, 15660.
(25) Shen, S. H.; Chen, X. B.; Ren, F.; Kronawitter, C. X.; Mao, S. S.; Guo, L. J. *Nanoscale Res. Lett.* **2011**, *6*, 290.

DOI: 10.1021/ic503101s
Inorg. Chem. 2015, 54, 2467−2473